IEEE Access
Multidisciplinary | Rapid Review | Open Access Journal

Received July 12, 2019, accepted August 2, 2019, date of publication August 6, 2019, date of current version August 21, 2019.

Digital Object Identifier 10.1109/ACCESS.2019.2933485

Design and Experiments for a Kind of Capacitive Type Sensor Measuring Air Flow and Pressure Differential

ZHANSHE GUO, TAIYI ZHANG, FUQIANG ZHOU, AND FENGPEI YU
School of Instrumentation and Optoelectronic Engineering, Beihang University, Beijing 100191, China

Corresponding authors: Taiyi Zhang (buaazhangty@163.com) and Fuqiang Zhou (zfq@buaa.edu.en)

This work was supported in part by the National Natural Science Foundation of China (NSFC) under Grant 61471123, and in part by the Beihang University Graduate Student Innovation and Practice Fund.

ABSTRACT A kind of capacitive type air flow sensor is designed and fabricated for respiratory flow measurement. Major sensitive elements of the sensor are two parallel placed capacitance plates which are perpendicularly fixed on the sidewall of the air channel. The flow and pressure differential of air can be calculated by measuring the change of the micro capacitance, which is initiated by air pressure. The Bernoulli equation and the continuous equation of the fluid are used for theoretical analysis. The mechanical analysis and FEM (finite element method) is used to make the optimum design for the sensor. Then, the micro capacitance measuring circuit using the so called peak detection method is fabricated and corresponding A/D convert digital circuit are also made. Experimental result indicates the capacitance measuring circuit has little error. The accuracy, sensitivity, and resolution of the circuit reach 0.2% FS, 1.4089 V/pF, 0.003 pF respectively, which indicates this kind of system is feasible in practical applications.

INDEX TERMS Capacitive type, pressure differential, air flow sensor, optimum design.

I. INTRODUCTION

Generally, the volume or mass of fluid flowing through a certain effective section per unit time, is called the flow through the section. The former is called volume flow and the latter is called mass flow. Mass flow sensors, which are mostly used for accurate measurement because of its insensitivity to some parameters such as temperature and pressure, can be divided into indirect and direct ones according to measurement methods [1]. Common direct flow sensors include thermal, Coriolis, and impulse mass flow sensors [2], within which the mostly used is the thermal mass flow sensor which has the benefit of large range, high accuracy, and high reliability. The thermal mass flow sensor measures the mass flow by detecting the transfer or dissipation of heat when the air is heated. Based on the heat transfer principle, the flow rate is measured by detecting the direct heat exchange relationship between the air in the pipeline and the flow sensor [1]. In 2016 [3], C. Wu *et al.* designed a MEMS thermal flow sensors with the dumbbell type, aiming at measuring liquid flow whose rate is down to 0.05 μl/min, and the sensor turned out to have a sensitivity of 7.7 mV/(μl/min). In 2017 [4], K. Clocker *et al.* presented a brand new architecture using a single, resistive transducer element to measure fluid flow with a two-phase control and measurement algorithm, and related experiments indicated that the architecture is feasible.

Volume flow sensors can be divided into speed type, volumetric and differential pressure type based on the sensitive mechanism. To differential pressure flow sensors, when the fluid flows through a throttling element, the flow velocity and kinetic energy of the fluid in the constricted cross section will increase rapidly as the cross-sectional area of the tube suddenly becomes smaller. Since the energy loss of the fluid in the contraction stage is very small, it can be assumed that the total energy is a constant. According to the law of conservation of energy, in the ideal case, the fluid is accelerated after the partial static pressure is converted into kinetic energy, in another word, the static pressure of the fluid is reduced [5], which generated differential pressure, and there is a certain functional relationship between this differential pressure and flow rate, so the value of flow rate can be obtained indirectly by measuring the differential pressure. In 2015 [6], P. Chen designed a kind of beam-membrane structure micromachined flow sensor, based on the principle of differential pressure

The associate editor coordinating the review of this manuscript and approving it for publication was Bora Onat.

caused by the mass flow, and the calibration results show that the beam-membrane structure differential pressure flow sensor achieves ideal static characteristics and works well in the practical applications. In 2016 [7], D. Bridgeman *et al.* presented a new differential pressure-based flow meter for human breath measurements, and characterized the new sensor flow experimentally and theoretically, by means of laminar and turbulent models in Comsol Multiphysics® Software. In addition, S. Pant *et al.* proposed a non-invasive, wearable, Fiber Bragg Grating Respiratory Measurement Device in 2018 [8].This device employs two FBG sensors to capture the respiratory cycle from both the nostrils of the subject. It comprises the ability to acquire the respiratory pattern employing the nasal airflow and the respiratory parameters will be obtained. In 2019 [9], I. Lorato *et al.* provides the proof-of-concept that low-cost thermopile-arrays can be used to monitor respiratory flow in a lab setting and the sensor has been proven to allow respiratory flow detection over a range of parameter settings.

By comparing all methods mentioned above, it can be concluded that indirect methods are relatively more sensitive to external factors due to their indirect measuring approaches. Currently, the standard method for measuring flow rate is to use a differential pressure orifice flowmeter. This method reflects the flow rate by measuring the gas pressure difference across the orifice, which is simple, universal and reliable. However, the measurement accuracy depends on the differential pressure gauge. The structure proposed in this paper is also similar to the throttling device. It is not necessary to measure the pressure differential directly, but to convert the pressure differential generated by the airflow into a change in capacitance. Capacitance detection is a kind of non-contact detecting method, it is not easily affected by the temperature, humidity and some other interference in some specific circumstances. Based on all of these, a new kind of capacitive type air flow sensor is designed and fabricated in this article. It has the advantages of low consumption, low cost and it is portable. Most importantly, it can realize the measurement of pressure differential and flow at the same time, which can be applied in respiratory flow measurement at normal temperature and pressure.

II. WORKING PRINCIPLE OF THE SYSTEM

The system is mainly composed of a tube through which air flows, a capacitance detection circuit, A/D conversion circuit and DSP (Digital Signal Processing) module. The core of the system is a tube with capacitance plates as throttling gears in it. One of the capacitance plates is thinner and its shape is easily changed by the air flow because of its low stiffness, while the other one is thicker and hardly deforms. Thus it is the sensitive element to respond to the air flow. The capacitance value changes regularly with the shape changing of capacitance plate according to pertinent theory. Then the capacitance detection circuit converts the capacitance signal to proportional voltage signal. A/D conversion circuit can realize the conversion of analog voltage signal into digital signal. Finally, a DSP section is used to process the acquired digital voltage signal and realize the calculation of flow and pressure differential. The using of DSP can improve the calculation speed, accuracy and realize real-time acquisition, which is an advantage of the sensor.

III. THEORY ANALYSIS AND OPTIMUM DESIGN OF THE SENSOR

The air flow sensor to some extent refers to the design of differential pressure flow sensors, so the sensor can get flow and pressure parameters differential in the same time. Some theoretical analysis of flow and pressure is necessary before the designation.

A. THEORY ANALYSIS OF FLOW IN PIPE

The air flow sensor consists of two parts, which are airflow tube and capacitance plates. Capacitance plates are set in the airflow and play the role of sensitive and throttling element. The simplified sketch map of the device is shown in Figure 1. The inlet is on the left, which is connected with section 1. The outlet is on the right and it is open to atmosphere. The pressure in section 1 is caused by respiration.

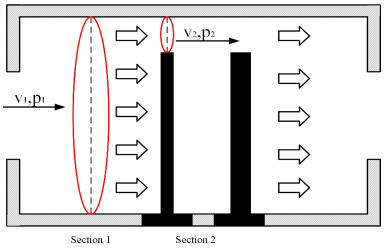

FIGURE 1. Schematic of airflow in pipeline.

According to fluid Bernoulli theory, when incompressible and ideal air flows through variable cross-section tube, its speed and pressure are changing with the change of cross-section area. The sum of kinetic energy, gravitational potential energy and pressure potential energy of fluid is fixed. When the flow rate of flow to be measured is low, it can be regarded as incompressible fluid and its viscosity can be neglected. So the Bernoulli equation can be expressed as:

$$gz + \frac{p}{\rho} + \frac{v^2}{2} = M \tag{1}$$

where g is the gravitational acceleration value, z is the height of vertical position, ρ is the density of fluid, v is the velocity of fluid, p is the pressure of fluid, M is a constant value. In this design, z changes little. So the equation may change into:

$$\frac{p}{\rho} + \frac{v^2}{2} = M \tag{2}$$

According to the continuous equation of fluid, the fluid can neither interrupt nor piled up when flowing through the pipe. In unit time, the quality of air flow through every cross section is the same. The status of the flow between the pipe of inlet

and the gap between capacitance plate and wall of tube can be described with the following equation:

$$\rho_1 v_1 s_1 = \rho_2 v_2 s_2 = m \tag{3}$$

where ρ_i is the density of fluid, v_i is the velocity of fluid, s_1 is the cross section area of the tube, s_2 is the cross section area of the throttling element, which includes the gap between the top of capacitive plate and the tube and the gap between the flank of capacitive plate and the tube, m is the quality of air which flow through the tube per second.

Refer to (2) and (3) the Bernoulli theory and continuous equation of fluid can be combined as the following equation.

$$\frac{1}{2}\rho_1 v_1^2 + p_1 = \frac{1}{2}\rho_2 v_2^2 + p_2 \tag{4}$$

where, v_1 and p_1 stand for the velocity and pressure in section1, respectively. v_2 and p_2 stand for the velocity and pressure in section2, respectively.

Thus the differential pressure between section 1 and 2 can be calculated as:

$$\Delta p = p_1 - p_2 = \frac{1}{2}\rho v_2^2(1 - \frac{s_2^2}{s_1^2}) = \frac{1}{2}\rho Q^2(\frac{1}{s_2^2} - \frac{1}{s_1^2}) \tag{5}$$

where Δp is the differential pressure between section 1 and section 2. This is also the pressure impacted on the capacitance plate. s_i is the cross section area in section i. Q(L/min) is the flow rate of air.

Equation (5) indicates that the pressure difference is proportional to the square of flow when the density of air land the structure of pipe and capacitance plate are fixed. In practical application, the actual orifice area is not completely equal to the cross-sectional area of section2(area difference between pipe and capacitance plate) due to the fact of pipe roughness, air density changes caused by the temperature and air compression after the orifice. In addition, considering the changes in air density caused by the temperature and air compression and the effect of vena contracta, the phenomenon that the cross section of air flow continues to shrink after the airflow passes through the orifice, the correction coefficient should be added after calibration and Δp is calculated by using (6).

$$\Delta p = \frac{1}{2}\zeta\rho v_2^2(1 - \frac{s_2^2}{s_1^2}) = \frac{1}{2}\zeta\rho Q^2(\frac{1}{s_2^2} - \frac{1}{s_1^2}) \tag{6}$$

If the structure of pipe and the size of throttling gears are certain, then the correction factor ζ can be got through calibration experiment.

When the cross-sectional area of section 2 is small, the density of the air in pipe will change and the gas will be compressed. The Bernoulli equation can be expressed as:

$$\frac{v_1^2}{2} + \frac{\kappa}{\kappa - 1}\frac{p_1}{\rho_1} = \frac{v_2^2}{2} + \frac{\kappa}{\kappa - 1}\frac{p_2}{\rho_2} \tag{7}$$

where κ is the isentropic exponent, which is 1.4 for air. According to (3) and (7), since the density of air increases after compression, the actual pressure differential is smaller than the result obtained from (6). However, in this case, the pressure and density changes of air are complicated and the relationship between pressure differential and flow rate cannot be directly derived from the formula. Therefore, the obvious compression of air should be avoided when we design the size of the throttling element.

B. THEORY ANALYSIS OF NON-PARALLEL CAPACITANCE CALCULATION METHOD

In this design, the original status of capacitor is two parallel plates. There will be deformation on the capacitance plate when air flowing through the tube. This will cause the change of clearance between two capacitance plates, which results in change of capacitance value. The calculation of capacitance value before and after air flow applying on is necessary to the designation of devices.

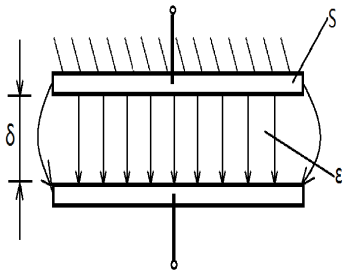

FIGURE 2. Structure of parallel plate capacitor.

Figure 2 shows the structure of parallel plate capacitor and the value of it can be calculated by the equation below.

$$C = \frac{\varepsilon S}{\delta} \tag{8}$$

where, δ(m) is the distance between parallel plates, S(m^2) is the area between two plates, ε is the dielectric constant of medium between parallel plates.

However, for our design, the capacitance plates are not always parallel to each other, so the model of capacitor with nonparallel capacitance plates are shown in Figure 3:

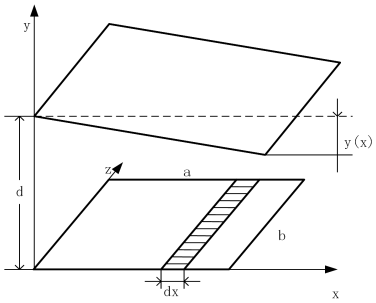

FIGURE 3. Nonparallel capacitance plates.

X-axis, Y-axis and Z-axis are also set in the model shown as Figure 3. When uniform pressure is applied on parallel capacitance plates, displacement of bottom clamped sensitive capacitance plate will occur. Then, the clearance of two

capacitance plates can be expressed as:

$$\delta = d - y(x) \tag{9}$$

where d is the initial clearance of two capacitance plates, $y(x)$ is the displacement of sensitive plate. The non-parallel capacitance plates could be divided into numerous small stretches. Based on calculating method of ideal capacitor with parallel capacitance plates, regarding the capacitance plates as countless micro sections, and each section corresponds to a capacitance value ΔC_i, then the value of whole capacitors can be expressed as:

$$C = \Delta C_1 + \Delta C_2 + \ldots + \Delta C_N = \frac{\varepsilon \Delta S_1}{\delta_1} + \frac{\varepsilon \Delta S_2}{\delta_2} + \ldots + \frac{\varepsilon \Delta S_N}{\delta_N} = \int_0^a \frac{\varepsilon b}{d - y(x)}\, dx \tag{10}$$

where, a and b are the length and width of capacitance plate, respectively.

The capacitance structure consists of two parallel plates. They are both fixed by one end in the pipe through which the air flows. One of the capacitance plates is much thinner than the other one, for it performs as the sensitive element reacting to air flow in pipe. The shape of thinner plate will change obviously while the thicker one changes little when air flow working on them. So the clearance between two parallel capacitance plates will change.

According to the theory of elastic mechanics, the equilibrium equation of a thin plate under uniform load which is expressed by the displacement $y(x, z)$ can be described with the following equation:

$$\frac{\partial^4 y(x,z)}{\partial x^4} + 2\frac{\partial^4 y(x,z)}{\partial x^2 y^2} + \frac{\partial^4 y(x,z)}{\partial z^4} = \frac{p(x)}{D} \tag{11}$$

where $y(x, z)$ is the displacement of the plate in the Y-axis direction at (x, z), $p(x)$ is the load, D is the flexural rigidity of the plate.

When the single-ended fixed capacitor plate is loaded, the plate becomes a cylindrical surface, and its bus bar is parallel to the Z-axis. Therefore the displacement function $y(x, z)$ is only related to x and the equilibrium equation degenerates to:

$$\frac{\partial^4 y(x,z)}{\partial x^4} = \frac{p(x)}{D} \tag{12}$$

The equilibrium differential equation of the beam can be expressed as:

$$\frac{\partial^4 y^*(x)}{\partial x^4} = \frac{p(x)}{EI} \tag{13}$$

where $y^*(x)$ is the displacement of beam, $p(x)$ is the load and EI is the flexural rigidity of beam. The above two equations are similar, so the cylindrical curvature of a plate can be solved analogously to the bending of a beam.

According to the theory of material mechanics, the displacement of a cantilever beam under uniform load can be calculated as:

$$y^*(x) = \frac{p(x)x^2}{24EI}(x^2 - 4lx + 6l^2) \tag{14}$$

where l represents the length of the beam. Similarly, the displacement of the capacitance plate can be calculated as:

$$y(x) = \frac{\Delta p x^2}{24D}(x^2 - 4ax + 6a^2) \tag{15}$$

where a is the length of the capacitance plate and Δp is the differential pressure, which is the uniform load of the plate.

Refer to (10) and (15), C can be expressed as:

$$C = \int_0^a \frac{\varepsilon b}{d - y(x)}\, dx = \int_0^a \frac{\varepsilon b}{d - \frac{\Delta p x^2}{24D}(x^2 - 4ax + 6a^2)}\, dx \tag{16}$$

The flexural rigidity D can be calculated as:

$$D = \frac{Eh^3}{12(1 - \upsilon^2)} \tag{17}$$

where E and υ represent the elastic modulus and Poisson's ratio of the capacitance plate material respectively, and h is the thickness of the plate.

C. DIMENSION DESIGN AND FEM SIMULATION OF DEVICE STRUCTURE

This section is aimed to determine the shape and dimension of the thinner capacitance plate. During the design of capacitance plate and tube, some rules must be obeyed as follows:

The initial clearance of two capacitance plates should be larger than the maximum displacement of the thinner plate when air flow works on it. Or the capacitance plates may cause short circuit. With the requirement of portability, the cross-section area of tube is set as 100 mm^2. In order to ensure air flows through the tube fluently, the cross-section area of capacitance plate should not surpass 90 mm^2. Considering the ideal cases, the area of capacitance plate can be regarded as throttling area in the tube. The shape and dimension design of capacitance plates should follow the following steps.

To begin with, using an appropriate material of capacitance plates is necessary due to the fact that different material has different characteristics. After times of tries, beryllium bronze is selected as the material of sensitive capacitance plate. The elastic modulus of the material is 128GPa, which is much smaller than steel and most of metal, which also means it is easier to deform than other metal materials. The Poisson's ratio is 0.35. In addition, this material possesses advantages of high corrosion resistance, fatigue limit and conductivity too.

Then, the initial clearance of two capacitance plates is needed. In order to set the initial clearance between two capacitance plates, the maximum deformation of capacitance plate under different flow rate is needed. For the same structure and dimension of plate, the greater the flow, the greater the pressure applied on the thinner plate, which means the

TABLE 1. Relationship between cross-section area and pressure.

Cross-section area(mm^2)	Pressure(Pa)
30	695
40	1187.7
50	2004
60	3507
70	6740
80	16034
90	66142

larger the deformation of it. The flow range of respiratory air of human is 0 to 200L/min, therefore, considering 200L/min as the biggest air flow, applied on the thinner plate to get the largest displacement of every structure. With fixed air density and cross-section area of tube, different pressure applied on different cross-section area of capacitance plates can be calculated from (5). The statistics are shown in Table 1.

As can be seen from Table 1, when the cross-section area of capacitance plate reaches $90mm^2$, the pressure differential is 66142Pa. In this situation, the air density will change significantly and the calculation of the pressure differential is not reliable. According to the theory of fluid dynamics, the compressibility of gas can be ignored when the Mach number of the airflow is less than 0.3. Taking the local sound velocity as 340m/s, then the gas compressibility is negligible when the air velocity in section 2 is less than 113m/s. Therefore, in order to avoid significant compression of the air in pipe, according to (3), s_2 should be more than $30mm^2$ and the cross-section area of capacitor plate should be less than $70mm^2$.

After that, FEM simulations of different models have been made to get the best structure and dimension of capacitance plates. The bottoms of the plates are fixed in the tube. The thinner plate senses the air flow, so FEM simulations of it are carried out. First we assume that the capacitor plate is square. The area of square plates changes from $30mm^2$ to $70mm^2$ and the thickness is 0.1mm. After five groups of simulation, results of square capacitance plates with different areas are listed in Table 2.

The minimum clearance should not be less than 0.5mm according to assembly technology. d_{smax} and s_{max} can be get from structural simulation of ANSYS. C_0 and ΔC can be calculated according to (8) and (16). From the statistics in table, the maximum displacement of each plate is smaller than the initial clearance and the maximum stress is lower than the fatigue limit of beryllium bronze. Considering the value of capacitance variation, processing difficulty and maximum stress applied on plate, areas from $40mm^2$ to $70mm^2$ are the best choice. In order to get the best dimension of capacitance plate, several groups of simulations with different aspect ratio are made with the thickness of 0.1mm and areas between $40mm^2$ to $70mm^2$. The statistics are shown in Table 3.

From the results, it can be concluded that the changing value of capacitor is lager when the height and width are 10mm and 6mm respectively, which means the structure has better sensitivity when sensing air flow. So the structure with rectangle cross-section and dimension with 6mm×10mm×0.1mm has been selected as sensitive capacitance plate, which is shown in Figure 4.

According to the results of FEM simulation, the color nephogram of displacement and stress are shown in Figure 5 and Figure 6, respectively.

It can be concluded from Figure 5 that the displacement of rectangle capacitance plate is well-proportioned horizontally with uniform pressure applied. Its displacement curves obtained by (15) and FEM simulation are shown in Figure 7, indicating that the results of mathematical model are consistent with the simulation results.

TABLE 2. Results of square capacitance plates with different areas.

$A(mm^2)$	Δp(Pa)	d_{tmax}(mm)	d_{smax}(mm)	s_{max}(MPa)	d_{ini}(mm)	C_0(pF)	ΔC(pF)[a]
70	6740	0.340	0.376	152.1	0.5	1.24	0.653
60	3507	0.130	0.139	66.3	0.5	1.06	0.133
50	2004	0.0515	0.0515	30.54	0.5	0.885	0.039
40	1188	0.0195	0.0204	24.36	0.5	0.708	0.011
30	695	0.0064	0.0068	6.491	0.5	0.531	0.003

[a] A is the area of the capacitance plate. Δp is the pressure applied on capacitance plate. d_{tmax} is the theoretical value of the maximum displacement of sensitive capacitance plate. d_{smax} is the simulated value of the maximum displacement of sensitive capacitance plate. s_{max} is the maximum stress of the plate.d_{ini} is the initial clearance of two parallel capacitance plates. C_0 is the origin value of capacitance.ΔC is the difference value between C_0 and the changed capacitance value.

TABLE 3. Results of rectangular capacitance plates with different aspect ratio.

$A(mm^2)$	Δp(Pa)	d_{tmax}(mm)	d_{smax}(mm)	s_{max}(MPa)	d_{ini}(mm)	C_0(pF)	ΔC(pF)
5 × 8	1188	0.050	0.053	24.5	0.5	0.709	0.030
5 × 9	1540	0.10	0.11	40.6	0.5	0.797	0.077
5 × 10	2004	0.21	0.22	65.9	0.5	0.886	0.202
6 × 8	2000	0.084	0.088	40.7	0.5	0.850	0.064
6 × 9	2498	0.17	0.18	65.2	0.5	0.957	0.166
6 × 10	3507	0.36	0.39	109	0.5	1.06	0.639
7 × 8	2782	0.12	0.12	56	0.5	0.992	0.110
7 × 9	4212	0.28	0.30	108	0.5	1.116	0.419
7 × 10	6740	0.69	0.73	217	1.0	0.620	0.341

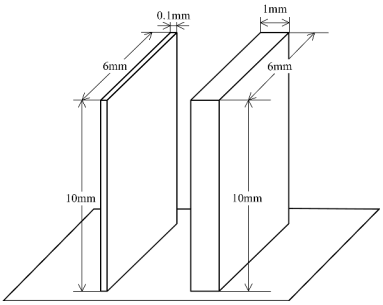

FIGURE 4. Sketch of rectangle capacitance plates.

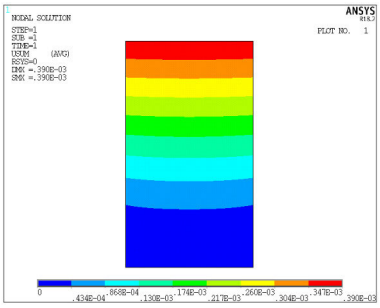

FIGURE 5. Displacement nephogram of capacitance plate (geometry dimensions of capacitance plates: 6mm × 10mm × 0.1mm unit of displacement: m).

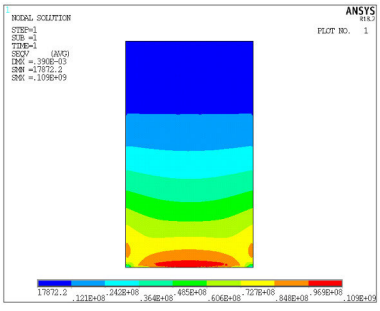

FIGURE 6. Stress nephogram of capacitance plate (geometry dimensions of capacitance plates: 6mm × 10mm × 0.1mm unit of stress: Pa).

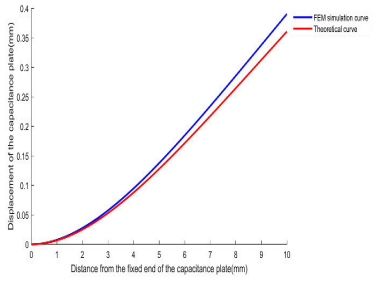

FIGURE 7. Displacement curve of capacitance plate.

The structure of tube has also been designed by AutoCAD after the dimension of plate is certain. The tube consists of pipeline and cover, which are shown as Figure 8 and Figure 9, respectively. The cross-section shape of tube is rectangle so that it matches the shape of capacitance plates well. Two ends

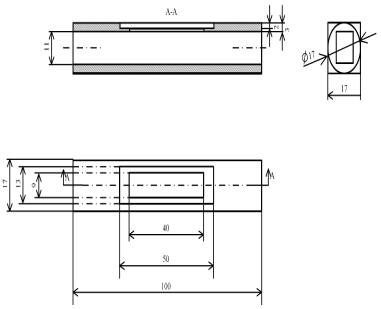

FIGURE 8. Pipeline of the tube(mm).

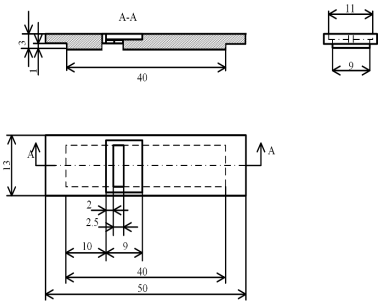

FIGURE 9. Cover of the tube(mm).

FIGURE 10. Manufactured device of the tube.

of tube are cylinder-shaped, which makes it easy to connect with breathing hosepipe. The clearance between two capacitance plates can be adjusted by hand. Manufactured device is shown in Figure 10.

D. THE RELATIONSHIP AMONG CAPACITANCE VARIATION, FLOW AND PRESSURE DIFFERENTIAL

When dimensions of capacitance plate and tube are fixed, ten groups of structural simulations are made with different pressures applied. With the dimensions of capacitance plate and tube, the pressure can be calculated by (6) with different flow. The relationship can be expressed as:

$$\Delta p = 0.088Q^2 \tag{18}$$

where, Q(L/min) is the flow rate of air. Δp(Pa) is the pressure applied on the plate. Simulations are made under different pressure and same initial clearance of 0.5mm. With the same method as before, the initial capacitance and capacitance after

TABLE 4. Relationship between air flow and ΔC.

Q(L/min)	Δp(Pa)	ΔC(pF)
0	0	0
20	35	0.003
40	142	0.013
60	316	0.029
80	561	0.053
100	880	0.087
120	1265	0.134
140	1722	0.197
160	2252	0.288
180	2847	0.421
200	3507	0.639

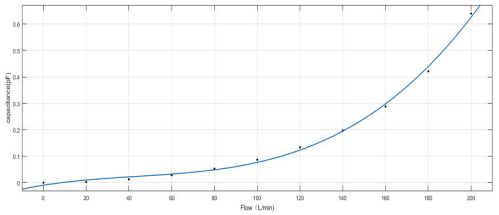

FIGURE 11. Curve of relationship between flow and ΔC.

changing can be calculated. Ten groups of statistics are shown in Table 4.

Figure 11 shows the curve of relationship between flow and ΔC.

The relationship is described by (19), which is given through polynomial fitting. Its correlation coefficient is 0.9974, which means the cubic polynomial function is a good model.

$$\Delta C = 1.363 \times 10^{-7} Q^3 - 1.782 \times 10^{-5} Q^2 + 0.001281 Q - 0.0090421 \quad (19)$$

where Q(L/min) is the flow rate of air flow. ΔC(pF) is the capacitance variation. The relationship between ΔC and Δp can be expressed as:

$$\Delta C = 5.221 \times 10^{-6} \Delta p^{1.5} - 2.025 \times 10^{-4} \Delta p + 4.328 \times 10^{-3} \Delta p^{0.5} - 0.0090421 \quad (20)$$

IV. DESIGN AND REALIZATION OF THE HARDWARE CIRCUIT BASED ON DSP AND CPLD

The circuit is designed to convert changing capacitance into voltage, which could be acquired and processed by digital signal processor. The circuit consists of four parts. They are carrier wave generation, C/V conversion, amplification circuit, peak detection and filter.

The improved Wien bridge circuit is used to generate the sine signal, which is used to realize the capacitance signal modulation. Schematic circuit diagram is shown in Figure 12:

The frequency of sine signal is depending on two RC nets (R2, C2 and R1, C1).

$$f_0 = 2\pi RC \quad (21)$$

where, $R_1 = R_2 = R$, $C_1 = C_2 = C$. Its amplitude can be adjusted by parameters of following circuit.

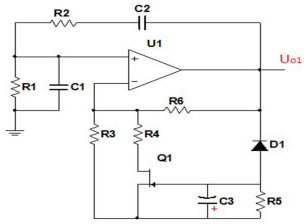

FIGURE 12. The improved Wien bridge circuit.

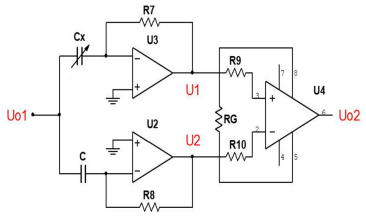

FIGURE 13. C/V conversion circuit.

C/V conversion circuit (see Figure 13) is aimed at convert capacitance signal into voltage signal, which consists of two amplifier circuits with same parameters. The output of one amplifier is the modulation signal of a fixed capacitance. The other is the modulation signal of changing capacitance which derives from the air flow sensor. Signals of these two channels can be expressed as ($R_7 = R_8 = R_f$):

$$U_1 = -R_f \times C_x \times \frac{dU_i}{dt} \quad (22)$$

$$U_2 = -R_f \times C \times \frac{dU_i}{dt} \quad (23)$$

An instrumentation amplifier is used in amplification circuit with input of two differential signal generated in C/V conversion circuit. According to the working principle of instrumentation amplifier, the output signal of it can be expressed as:

$$U_{o2} = G(U_1 - U_2) \quad (24)$$

where G is the amplification factor.

$$G = 1 + \frac{50k}{R_G} \quad (25)$$

Supposing $\Delta C = C_x - C$, then:

$$U_{o2} = G(U_1 - U_2) = -\Delta C \times R_f \times (1 + \frac{50k}{R_G}) \times \frac{dU_i}{dt} \quad (26)$$

Peak detection circuit (see Figure 14) is used to realize the demodulation of signal. The output signal of peak detection is U_{o3}, which is the amplitude of U_{o2}. The filter circuit, consists of a first-order filter, is aimed at reducing the high frequency noise. Then, the voltage signal U_o which is proportional to capacitance changing can be obtained.

In order to suppress the electromagnetic interference, we set appropriate frequency carrier wave, design the filter circuit to reduce high-frequency interference, isolate the signal source and subsequent circuits with the voltage follower,

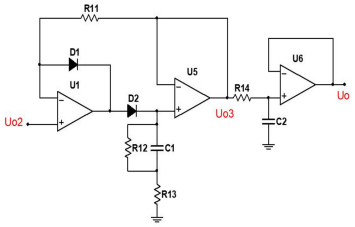

FIGURE 14. Peak detection circuit.

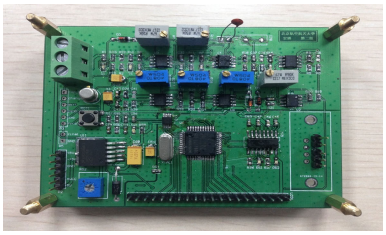

FIGURE 15. Actual picture of the testing circuit.

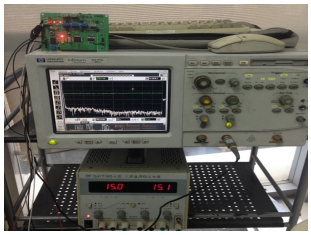

FIGURE 16. Calibration experiment.

and arrange the wiring reasonably when designing the PCB board. The circuit board is shown in Figure 15.

V. EXPERIMENT

From the analysis of Sec. III D, it turns out that there exists a good functional relationship between ΔC (pF) and Q(L/min), so the performance of capacitance detecting can also reflect the performance of air flow measuring.

A. CALIBRATION EXPERIMENT OF ANALOG CIRCUIT

Fix-valued ceramic capacitors ($1-10$pF) are used as changing capacitances in circuit for calibration experiment of analog circuit. To get the real value of the ceramic capacitors, high precision LCR testing device whose model number is AH2770, is used as standard equipment for capacitance testing.

Group of experiments are made with different value of ceramic capacitors (see Figure 16). And the experiment results are shown in Table 5:

The relationship between output voltage and capacitance value can be plotted as Figure 17.

The relationship can be derived from linear regression as follows:

$$U = 1.4089\Delta C + 1.4297 \tag{27}$$

Its linear regression coefficient is 0.9999, which represents the good linear relationship of two parameters.

TABLE 5. Relationship between capacitance value and output voltage.

ΔC(pF)	U(V)	ΔC(pF)	U(V)
1.03	2.890	5.08	8.630
1.18	3.078	5.15	8.680
1.43	3.435	5.34	8.951
1.77	4.010	5.43	9.069
2.29	4.625	5.57	9.280
2.37	4.760	5.72	9.481
2.45	4.871	5.83	9.650
2.58	5.030	5.99	9.873
2.64	5.138	6.14	10.10
2.78	5.336	6.21	10.18
2.92	5.530	6.39	10.41
3.21	5.941	6.47	10.56
3.40	6.210	6.58	10.70
3.69	6.611	6.71	10.88
3.82	6.799	6.90	11.14
4.08	7.172	7.08	11.41
4.21	7.356	7.25	11.65
4.45	7.690	7.31	11.72
4.67	8.005	7.48	11.98
4.87	8.286	7.89	12.56

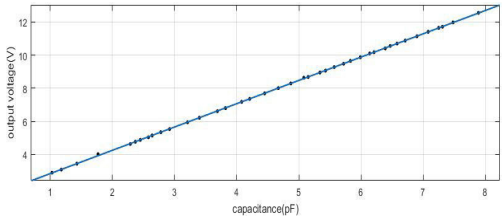

FIGURE 17. Relationship between output voltage and capacitance value.

TABLE 6. Measurement results of capacitors.

C_1(pF)	C_0(pF)	$Error(\%)$
1.950	1.954	0.2047
2.058	2.062	0.1940
2.241	2.245	0.1781
2.332	2.336	0.1712
2.640	2.635	0.1897
2.853	2.849	0.1404
3.032	3.029	0.0991
3.266	3.260	0.1840
3.544	3.538	0.1695
3.945	3.938	0.1777

B. PERFORMANCE TEST OF THE CIRCUIT

In this part, C_2 of the differential capacitance is fixed in advance and C_1 can be calculated by following equation:

$$C_1 = \frac{U - 1.4297}{1.4089} + C_2 \tag{28}$$

Then comparing our results C_1 with C_0 which is detected by high precision LCR testing device, and 10 groups of experiments are made, whose results are shown in Table 6.

1) ACCURACY

Accuracy refers to the relative error between the measured value and the true value, it can be seen from the last column in Table 6 that the accuracy reaches 0.2%.

2) SENSITIVITY

The sensitivity of detecting circuit means variation of the output voltage caused by the change of input capacitance per

TABLE 7. Result of resolution test.

C(pF)	U(V)	C(pF)	U(V)
2.625	2.305	2.842	2.616
2.635	2.327	2.904	3.708
2.636	2.327	2.905	3.708
2.639	2.331	2.907	3.711
2.734	2.466	2.914	3.719
2.738	2.471	3.005	2.848
2.745	2.481	3.008	3.853
2.760	5.498	3.009	3.852
2.763	2.503	3.012	3.859
2.770	2.515	3.015	3.864

FIGURE 18. Bell gas flowmeter.

unit, which can be expressed by equation below according to (27):

$$S = \frac{dU_o}{d\Delta C} = 1.4089V/pF \tag{29}$$

3) NONLINEAR

According to our data, the maximum value between output voltage and ideal voltage is 0.086V, and the range of output voltage is 9.67V, so the nonlinear of detecting circuit can be calculated:

$$\xi = \frac{\Delta U_{max}}{U_{max} - U_{min}} = 0.92\% \tag{30}$$

4) RESOLUTION

Resolution test experiments are also carried out, during the experiments, the fixed capacitance was set 2pF, and results are shown in Table 7.

It turns out that when the value of capacitors changes 0.003pF or more, the output voltages can be detected, which means the resolution of the circuit is 0.003pF.

C. CALIBRATION EXPERIMENT OF THE SENSOR

The calibration experiment was carried out in China metrology institute and the calibration device is shown in the Figure 18.

A steady flow of air was introduced into the pipeline and the sensor was calibrated by bell gas flowmeter. The experiment results are shown in Table 8.

Where Q(L/min) is the flow rate of air, U(V) is the output voltage. The relationship between them is obtained by cubic

TABLE 8. Result of calibration experiment.

Num.	Q(L/min)	U(V)
1	0	1.571
2	23.10	1.588
3	43.34	1.621
4	62.96	1.679
5	81.16	1.748
6	98.90	1.830
7	119.88	1.942
8	140.40	2.080
9	158.18	2.229
10	178.4	2.411
11	196.08	2.586

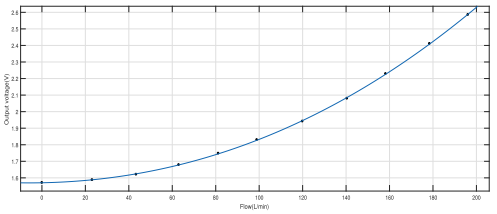

FIGURE 19. Relationship between flow and output voltage.

polynomial fitting:

$$U = 1.547 \times 10^{-8}Q^3 + 2.214 \times 10^{-5}Q^2 + 2.54 \times 10^{-4}Q + 1.57 \tag{31}$$

Figure 19 shows the curve of relationship between flow and output voltage.

VI. CONCLUSION

A kind of capacitive type air flow sensor is designed and fabricated for respiratory flow measurement in the article.

Firstly, theoretical analysis of the relationship between flow and pressure differential have been made, using the Bernoulli equation and continuous equation of fluid. The mechanical analysis and FEM simulation is used to make the optimum design for the sensor.

Secondly, to understand the change of capacitance value of the plat caused by the pressure generated by air flow, the micro capacitance measuring circuit using the so called peak detection method is fabricated.

Then the relationship among capacitance variation, flow and pressure differential was fixed through simulation and polynomial fitting, after that, the air flow and pressure differential can be calculated when ΔC is detected by the circuit.

Finally, calibration experiment was carried out to test the analog circuit, and result indicated that the micro capacitance measuring circuit has little error, and the performance test of the circuit showed that the accuracy, sensitivity and resolution of circuit reach 0.2%FS, 1.4089V/pF, 0.003pF respectively, which indicates this kind of system is feasible in practical applications.

REFERENCES

[1] H. Zhang, Y. Li, M. Zhong, M. Li, W. Guo, and Y. Liu, "A novel soft intelligent calibrator for low-velocity hot bulb anemometers," in *Proc. IEEE Int. Conf. Adv. Intell. Mechatronics (AIM)*, Jul. 2015, pp. 1597–1602.

[2] M. B. Gerdroodbary, M. Mosavat, D. D. Ganji, M. Taeibi-Rahni, and R. Moradi, "Application of molecular force for mass analysis of Krypton/Xenon mixture in low-pressure MEMS gas sensor," *Vacuum*, vol. 150, pp. 207–215, Apr. 2017.
[3] C.-H. Wu, D. Kang, P.-H. Chen, and Y.-C. Tai, "MEMS thermal flow sensors," *Sens. Actuators A, Phys.*, vol. 241, pp. 135–144, Apr. 2016.
[4] K. Clocker, S. Sengupta, M. Lindsay, and M. L. Johnston, "Single-element thermal flow sensor using dual-slope control scheme," in *Proc. IEEE Sensors*, Oct./Nov. 2017, pp. 1–3.
[5] J. P. Leitzke and H. Zangl, "Wireless differential pressure measurement for aircraft," in *Proc. IEEE Int. Workshop Metrology Aerosp. (MetroAeroSpace)*, Jun. 2017, pp. 164–168.
[6] P. Chen, Y. L. Zhao, B. Tian, C. Li, and Y. Y. Li, "A beam-membrane structure micromachined differential pressure flow sensor," *Rev. Sci. Instrum.*, vol. 86, no. 4, Apr. 2015, Art. no. 045004.
[7] D. Bridgeman, F. Tsow, X. Xian, and E. S. Forzani, "A new differential pressure flow meter for measurement of human breath flow: Simulation and experimental investigation," *AIChE J.*, vol. 62, no. 3, pp. 956–964, Mar. 2016.
[8] S. Pant, S. Umesh, and S. Asokan, "Fiber Bragg grating respiratory measurement device," in *Proc. IEEE Int. Symp. Med. Meas. Appl. (MeMeA)*, Jun. 2018, pp. 1–5.
[9] I. Lorato, T. Bakkes, S. Stuijk, M. Meftah, and G. De Haan, "Unobtrusive respiratory flow monitoring using a thermopile array: A feasibility study," *Appl. Sci.*, vol. 9, no. 12, p. 2449, Jun. 2019.

ZHANSHE GUO received the B.S. degree from the Changchun University of Science and Technology, in 1997, and the M.S. and Ph.D. degrees from the Changchun Institute of Optics, Fine Mechanics and Physics, Chinese Academy of Sciences, in 2000 and 2003, respectively.

He is currently an Associate Professor with the School of Instrumentation and Optoelectronic Engineering, Beihang University. His current research interests include advanced sensor technology and microelectromechanical systems.

TAIYI ZHANG received the B.S. degree from Beihang University, in 2017.

Her current research interest includes microelectromechanical systems.

FUQIANG ZHOU received the B.S., M.S., and Ph.D. degrees in instrument, measurement, and test technology from Tianjin University, Tianjin, China, in 1994, 1997, and 2000, respectively.

He joined the School of Automation Science and Electrical Engineering, Beihang University, Beijing, China, as a Postdoctoral Research Fellow, in 2000, where he is currently a Professor with the School of Instrumentation and Optoelectronic Engineering. His current research interests include computer vision and image processing.

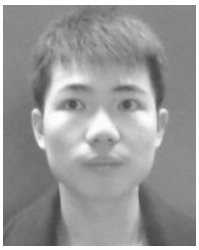

FENGPEI YU received the B.S. degree from Beihang University, in 2017.

His current research interests include signal acquisition and processing.